

## Supplementary materials

### **Neutrophils Affinity PGP and HAIYPRH (T7) Peptide Dual-ligand Functionalized Nanoformulation Enhanced Brain Delivery of Tanshinone IIA and Exerts Neuroprotective Effects Against Ischemic Stroke by Inhibiting Proinflammatory Signaling Pathways**

Yutao Li <sup>a 1</sup>, Danan Han <sup>a 1</sup>, Fengjin Li <sup>b</sup>, Yanxin Dang <sup>a, c</sup>, Xin Liu <sup>a, d \*</sup>,  
Fengming Zhang <sup>a</sup>, Yuan Xu <sup>d</sup>, Haijing Zhong <sup>d</sup>, Xiaojun Sun <sup>a \*</sup>

<sup>a</sup> Department of Pharmaceutical Engineering, School of Chemical and Environmental Engineering, Key Laboratory of Green Chemical Engineering, Harbin University of Science and Technology, Harbin, 150040, P. R. China

<sup>b</sup> Institute of Chinese Medicine, Heilongjiang Academy of Traditional Chinese Medicine, Harbin, 150036, China

<sup>c</sup> Heilongjiang Province Rehabilitation Hospital, Harbin, 150070, China

<sup>d</sup> Department of Pharmacology, School of Medicine, Yale University, New Haven, Connecticut, 06520, United States

\* Corresponding author

\*\* Corresponding author

E-mail address: xinliu98@126.com (X. Liu); sunxiaojun361@163.com (X. Sun)

1 Yutao Li and Dandan Han contributed equally to this work

## **1. Abbreviations:**

TS II A, tanshinone IIA; BBB, blood-brain barrier; PEG, polyethylene glycol; PAMAM, poly amidoamine; T7, HAIYPRH transferrin receptor-mediated peptide; PGP, N-acetylated proline-glycine-proline; PGP-T7-PEG-PAMAM NPs, PGP and T7 peptide dual-modified PEG-PAMAM nanoformulation; MCAO, Middle cerebral artery occlusion; IL, interleukin; IRAK, interleukin-1 receptor associated kinase; TRAF, TNF receptor-associated factor; TRAM, Toll-like receptor adaptor molecule; TRIF, Toll receptor associated activator of interferon; TTC, 2, 3, 5-triphenyltetrazolium chloride; TUNEL, terminal deoxynucleotidyl transferase (TdT)-mediated dUTP-biotin nick end labeling; DAB, 3, 3'-diaminobenzidine

## **2. Materials and methods**

### **2.1 Synthesis and Characterization of G 5.0 PAMAM Dendrimer**

G 5.0 PAMAM dendrimer was created according to the situ branch cell method mentioned in the previous reports, which is a two-step iterative process for constructing PAMAM dendrimers possessing either terminal ester or amine groups. This method includes (1) first step: alkylation with methyl acrylate (MA); (2) secondly, amidation with ethylenediamine (EDA).

The reactants were repeatedly washed with methanol (once every 2 h) and evaporated under reduced pressure at 40°C for 8 h to remove the methanol solvent and excess MA. After vacuum distillation, the crude product dissolved in 15 ml of methanol was extracted with 15 ml of anhydrous ether and centrifuged at 6000 rpm for 10 min. The obtained supernatant was washed with methanol and evaporated under reduced pressure to remove ether and methanol for obtaining a higher purity of G 0.5 PAMAM. The product of G 0.5 PAMAM was obtained with the yield of 98.7%.

Then, G 0.5 PAMAM methanol solution was added into a dried three-necked glass flask under the protection of nitrogen and magnetic stirring. The calculated amount of EDA was slowly dropped through dropping funnel under ice bath followed by subsequent reaction in the dark for 12 h. The reactants were repeatedly washed with methanol and evaporated under reduced pressure at 40°C for 8 h to remove the

methanol solvent and excess MA, and the pale yellow viscous liquid was obtained. G5.0 PAMAM dendrimers were synthesized through repetitive Michael addition and amidation condensation reaction. The yield of G5.0 PAMAM reached 99.7%.

The  $^1\text{H}$  NMR and  $^{13}\text{C}$  NMR spectra of G5.0 PAMAM dendrimer (dissolved in  $\text{D}_2\text{O}$ ) were analyzed in Bruker AVANCE 500 MHz NMR spectrometer (Switzerland). The sample of G5.0 PAMAM was ground, mixed with KBr and pressed into pellets. The infrared spectra were recorded in the spectral range of  $400\sim 4000\text{ cm}^{-1}$ , using a Nicolet 5700 FT-IR spectrometer with a resolution of  $2\text{ cm}^{-1}$ .

## **2.2 Cytotoxicity assay *in vitro***

The cytotoxicity of synergistic dual-targeting nanoformulation and single-ligand modified nanocarriers on brain capillary endothelial cells (BCECs) were evaluated by MTS assay using G5.0 PAMAM NPs and PEG-PAMAM NPs as control groups. On this purpose, an MTS test using CellTiter 96® Aqueous One Solution kit (Cell Proliferation Assay, Promega, USA) was performed. The test was executed on BCECs cell line. Cells were seeded in a 96-well plate,  $3\times 10^3\sim 5\times 10^3$  cells/well. An equal volume of NPs suspensions, at increasing concentrations from  $0.01\text{ }\mu\text{g/ml}$  to  $1000\text{ }\mu\text{g/ml}$ , was added to the cell culture media (DMEM, 10% FBS) and incubated for 48 h at  $37^\circ\text{C}$ , 5%  $\text{CO}_2$ . The results of cell survival profile were expressed as a percentage of vital BCECs cells with respect to control (cells incubated without NPs).

## **2.3 Stability and Drug Release**

To evaluate the stability of T7-PGP-TS II A-PEG-PLGA NPs, three PBS solutions (0.1 M, pH 5.0, pH 7.4 or pH 9.0) were prepared. 10 mg T7-PGP-TS II A-PEG-PAMAM NPs were suspended in 15 mL of each PBS solution with continuous stirring under 120 rpm at  $37^\circ\text{C}$ . The size and zeta potential of T7-PGP-TS II A-PEG-PLGA NPs were measured by dynamic light scattering (DLS) on days 0, 1, 2, 3, and 5 to monitor its stability <sup>1</sup>.

Cumulative tanshinone IIA release from T7-PGP-TSIIA-PEG-PAMAM NPs was determined by dispersing  $1\text{ mg/ml}$  of the NPs in 0.01 M phosphate buffer (pH 7.4),

and incubating it at 37°C. Aliquots of the dispersion were withdrawn at 0 min, 15 min, 30 min, 1 h, 2 h, 4 h, 8 h, 12 h, 24 h, 48 h and 72 h, and centrifuged at 15,000 rpm for 25 min. Volume of the dispersion withdrawn was replaced with fresh phosphate buffer. The supernatant was collected and TSIIA concentrations were quantitated by HPLC. The experiments were performed in triplicates.

#### **2.4 Pharmacokinetics and Biodistribution of the Dual-targeting TSIIA-encapsulated Nanoformulation**

Free TSIIA (10 mg/kg) suspended in CMC-Na solution (0.5%, w/v) T7-TSIIA-PEG-PAMAM NPs, PGP-TSIIA-PEG-PAMAM NPs and T7-PGP-TSIIA-PEG-PAMAM NPs (containing TSIIA, 10 mg/kg) dispersed in saline solution were administered to each group through the tail vein injection at a single dose, respectively. Around 200 µL of blood was collected from the jugular vein into heparinized centrifuge tube at predetermined time points (5, 15, 30, and 45 min; 1, 2, 4, 6, 8, 12, 24 and 36 h). The plasma was prepared for HPLC-MS/MS by removing protein with a precipitation method <sup>2</sup>. The prepared samples were kept in an auto-sampler at 4°C until injection, at which time 10 µL of supernatant fluid was injected into the HPLC/MS/MS system.

The UPLC-MS/MS system consists of Waters ACQUITY UPLC system (Waters Corp., Milford, MA, USA) and Waters Synapt™ High Definition TOF Mass system spectrometer (Waters Corp., Milford, USA). The data was collected and processed using MarkerLynx software MassLynx™ V 4.1 software with QuanLynx™ program (Waters Corp., Milford, MA, USA). Pharmacokinetic parameters were assessed by the software program DAS (version 2.1). The area under the curve of concentration vs. time (AUC) from zero to the last time point was calculated by the log-linear trapezoidal method.

In tissue distribution study, SD rats were sacrificed at predetermined time points, and then the brain tissue and other major organs including heart, liver, spleen, lung, brain and kidney were excised, followed by quick washing with cold saline to remove surface blood and stored at - 20°C until analysis. Briefly, tissues were homogenized in

ice saline, and then extracted three times with acetic ether. The organic phase was combined after centrifugation at 14,000 rpm for 10 min, and dried under a stream of nitrogen at 37°C. The dry residues were dissolved in 100 µL methanol, and the concentration of TSIIA was determined by the UPLC-QTOF-MS for analysis.

## **2.5 Induction of cerebral ischemia/reperfusion injury**

Briefly, the right common carotid artery (CCA), external carotid artery (ECA) and internal carotid artery (ICA) were isolated via a ventral midline incision. Branches of ECA were cauterized. The ECA was ligated and cut off at the distance of 5 mm from crotch of CCA. A nylon monofilament ( $\phi$  0.22~0.24 mm) with a rounded tip was inserted into right ICA about 18~20 mm through the broken end of ECA, until laser Doppler flow metry as an abrupt 80%~90% reduction of cerebral blood flow, indicating the occlusion of the origin of middle cerebral artery. Sham-operated control rat received the same procedure except filament insertion. After 2 h of ischemia, the nylon suture was withdrawn to establish reperfusion.

Rats were randomly divided into 7 groups (n = 6): group 1: sham-operated group injected with normal saline in a comparable volume; group 2: model group; group 3: vehicle control group administered with blank T7-PGP-PEG-PAMAM NPs dissolved in normal saline; group 4: treated with free TSIIA (10 mg/kg); group 5: treated with T7-TSIIA-PEG-PAMAM NPs (every day at a dose equivalent to 10 mg/kg of TSIIA for a total of 3 days); group 6: treated with PGP-TSIIA-PEG-PAMAM NPs (every day at a dose equivalent to 10 mg/kg of TSIIA for a total of 3 days) and group 7: treated with T7-PGP-TSIIA-PEG-PAMAM NPs (every day at a dose equivalent to 10 mg/kg of TSIIA for a total of 3 days). All formulations were administered *via* the intravenous route at the time of reperfusion following 2 h of ischemia/reperfusion, respectively.

## **2.6 Assessment of neurological function and infarct ratio**

After 24 h of reperfusion, neurological function assessment was carried out by an examiner blinded to the experimental groups, all of the rats from each group (n = 6) were assessed on a modified scoring system that developed from our previous studies

<sup>3, 4</sup>, as follows: 0, normal spontaneous movements; 1, difficulty in fully extending the contralateral forelimb; 2, unable to extend the contralateral forelimb; 3, mild circling to the contralateral side; 4, severe circling to the contralateral side; 5, an animal was unresponsive to noxious stimulus or unconsciousness.

Infract volume was determined by 2, 3, 5-triphenyltetrazolium chloride (TTC) after the neurological assessment (n = 6 per group). Animals were euthanized and the brains quickly collected. Brain tissue was sliced into 1 mm-thick coronal sections, stained with a 2% solution of TTC at 37°C for 30 min, followed by fixation with 4% paraformaldehyde <sup>4</sup>. Normal tissue was stained deep red, while the infract area was stained a pale gray color. TTC-stained sections were photographed and the digital images were analyzed using image analysis software (Image-Pro Plus 5.1, USA) to calculate the infarct ratio (%).

### **3. Results**

#### **3.1 Characterization of synergistic dual-targeting nanoformulation**

In <sup>1</sup>H NMR spectrum (Figure S2), the solvent peak of D<sub>2</sub>O was found at 4.691 ppm. The multiple peaks between 2.3 and 3.2 ppm belonged to the methylene protons of branching units of PAMAM. The proton of terminal amino group presented the corresponding peak at 2.327 ppm (Figure S2). The characteristic peak of -CH<sub>2</sub> connected with -CH<sub>2</sub>-CH<sub>2</sub>-NH<sub>2</sub>- corresponded to 3.235 ppm (Figure S2). The <sup>13</sup>C NMR data (Figure S3) shows a single peak of at 174.96/174.51 ppm attributed to the C=O in PAMAM dendrimer. The single peak at δ (ppm) 32.95 belonged to the carbon atom in -CH<sub>2</sub>- connected with the nitrogen of the -CH<sub>2</sub>-CH<sub>2</sub>-CONH- group (Figure S3). The characteristic peaks at δ (ppm) 38.67 and δ (ppm) 39.91 in the <sup>13</sup>C NMR spectrum of PAMAM (Figure S3) belonged to the carbon atoms in -CH<sub>2</sub>-NH- group. In FT-IR spectrum (Figure S4), the signal at 3288.68 cm<sup>-1</sup> belonged to stretching vibration peak of -NH<sub>2</sub> belonging to G5.0 PAMAM. The peaks at 2940.68 cm<sup>-1</sup> and 2867.74 cm<sup>-1</sup> were the asymmetric stretching vibration and symmetric stretching vibration of -CH<sub>2</sub>, respectively. The peak at 1638.01 cm<sup>-1</sup> pertained to the amide bond, the peak at 1560.34 cm<sup>-1</sup> is the stretching vibration of N-H bond and C-H bond in the amide bond; the peak at 1466.52 cm<sup>-1</sup> corresponded to the bending vibration of -CH<sub>2</sub>.

The peaks at 1198.74  $\text{cm}^{-1}$  and 1127.36  $\text{cm}^{-1}$  are the stretching vibrations of primary and tertiary amines, respectively. From the above data can be inferred, significant FT-IR spectral changes were detected in the region 1000~4000  $\text{cm}^{-1}$  containing  $-\text{NH}_2$ ,  $-\text{CONH}$ ,  $-\text{CH}_2-$ , C-N, tertiary amine and other functional characteristic groups, which consistent with the theoretical structure of G5.0 PAMAM. The  $^1\text{H}$  NMR,  $^{13}\text{C}$  NMR and FT-IR spectra (Figure S2, Figure S3 and Figure S4) demonstrated that the G5.0 PAMAM dendrimer were successfully synthesized.

The successful synthesis of PEG-PAMAM diblock copolymers was confirmed by the appearance of a signal at 3.578 ppm ( $^1\text{H}$  NMR) that corresponded to the methylene protons of NHS-PEG<sub>3400</sub>-MAL (Figure S5). In  $^{13}\text{C}$  NMR spectrum (Figure S6), the peaks at 175.50/174.67 ppm pertained to C=O group of PAMAM segment, and the methene group ( $-\text{CH}_2-$ ) of PEG segment appeared at 69.68 ppm. It can be seen from thin layer chromatography (Figure S7) that PEG-PAMAM has high purity and no impurity spots, indicating that there was no free NHS-PEG<sub>3400</sub>-MAL in PEG-PAMAM solution. As shown in FT-IR spectrum (Figure S8), PEG-PAMAM showed its unique characteristic peaks in the region from 1400  $\text{cm}^{-1}$  to 1100  $\text{cm}^{-1}$ . Furthermore, the stretching peak of primary amines near 1198  $\text{cm}^{-1}$  attributed to G5.0 PAMAM disappeared, and a new peak was observed at 3429.32  $\text{cm}^{-1}$ . This new peak was just the primary amino peak of G5.0 PAMAM present at 3288.68  $\text{cm}^{-1}$  (Figure S8) and red-shifted to 3439.32  $\text{cm}^{-1}$  in IR spectrum of PEG-PAMAM (Figure S8). The peak at 2918.13  $\text{cm}^{-1}$  was the stretching vibration peak of  $-\text{CH}_2$  belonged to PEG-PAMAM, and that at 1647.80  $\text{cm}^{-1}$  was the stretching vibration peak of carbonyl (C = O) attributed to PAMAM. The peak at 1458.34  $\text{cm}^{-1}$  is the bending vibration peak of  $-\text{CH}_2$  group in PAMAM, and the peak at 1101.92  $\text{cm}^{-1}$  is the stretching vibration peak of C-O-C in PEG. So it can be concluded that NHS-PEG<sub>3400</sub>-MAL reacted with the primary amino groups on the surface of G5.0 PAMAM. From the  $^1\text{H}$  NMR spectra of T7-PGP-TSIIA-PEG-PAMAM NPs (Figure S9), we observed that the repeat units of PEG presented a sharp peak at 3.7 ppm, showing that the MAL group had reacted with the thiol group of T7 and PGP <sup>5, 6</sup>. Finally, significant spectral changes are

detected in 3.724 ppm, 3.822 ppm, 3.953 ppm (Figure S9) assigned to the corresponding peaks of T7. The peaks around 6.826 ppm, 7.574 ppm and 7.671 ppm represented the protons in PGP histidine units, indicating the existence of PGP peptide (Figure S9) <sup>6</sup>. The <sup>1</sup>H NMR spectra results proved the existence of the conjugate structure of T7-PGP-PEG-PAMAM.

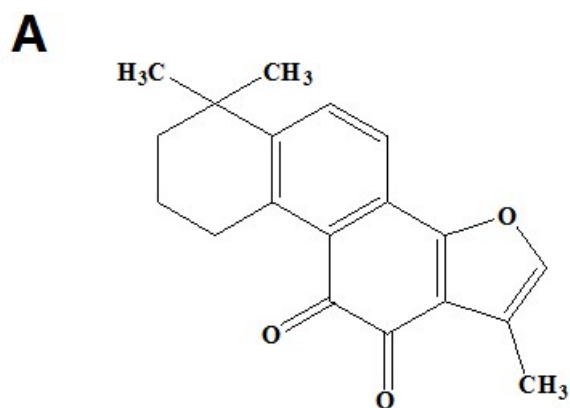


**Figure S1.** Chemical structure of tanshinone IIA (TS II A)



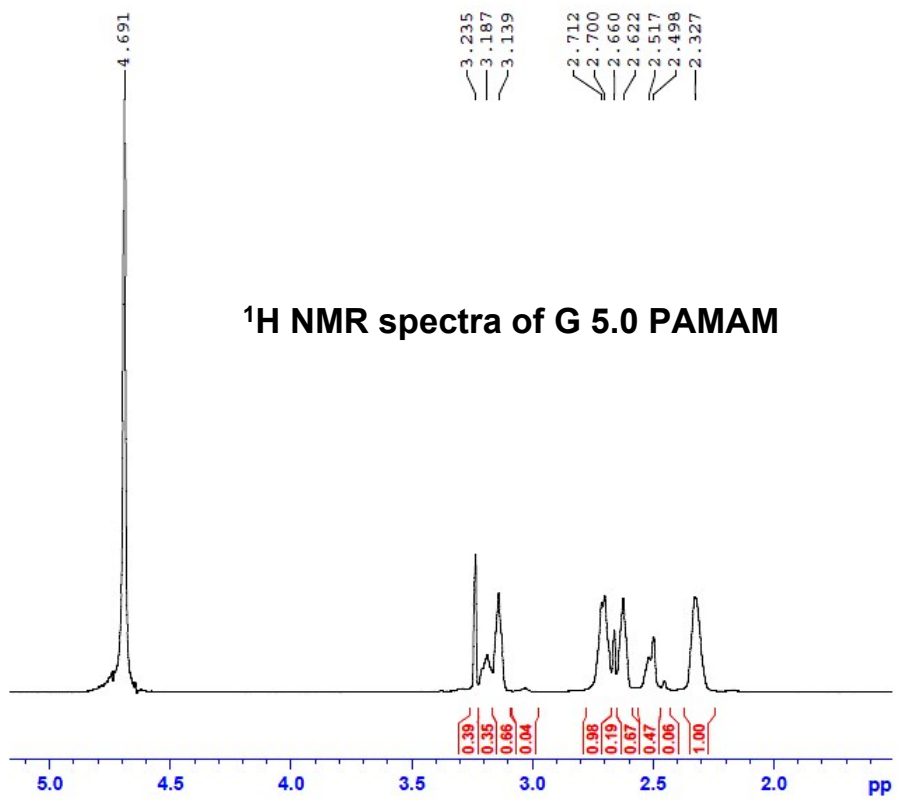


**Figure S2** <sup>1</sup>H NMR spectra of G 5.0 PAMAM

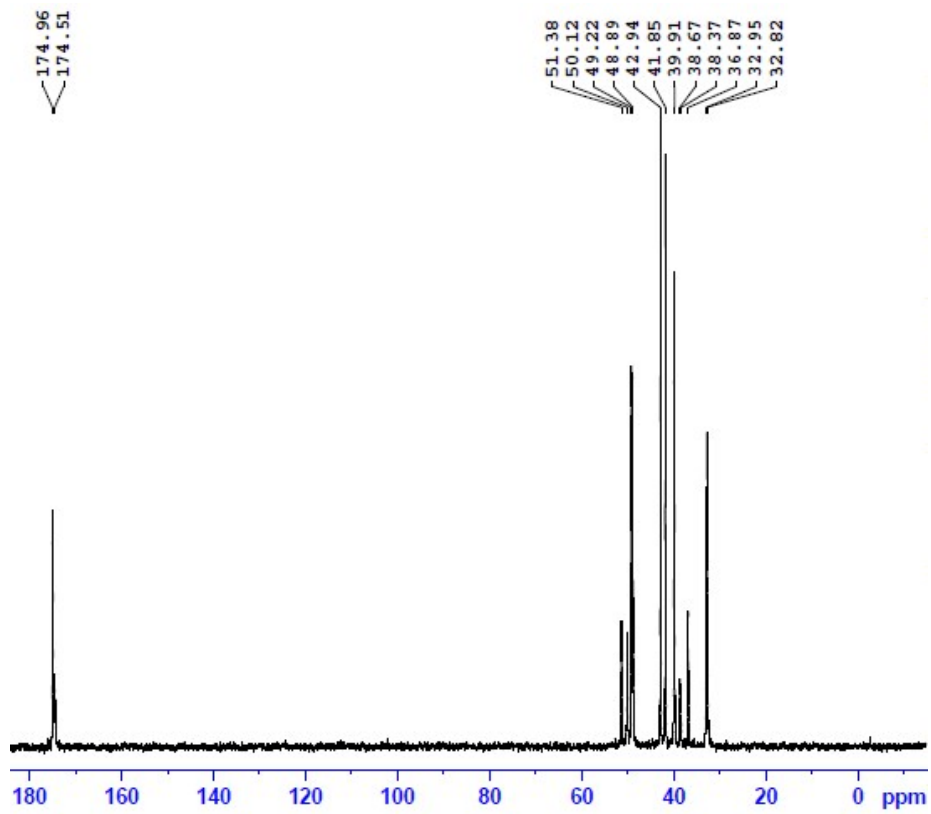


Figure S3  $^{13}\text{C}$  NMR spectra of G5.0 PAMAM

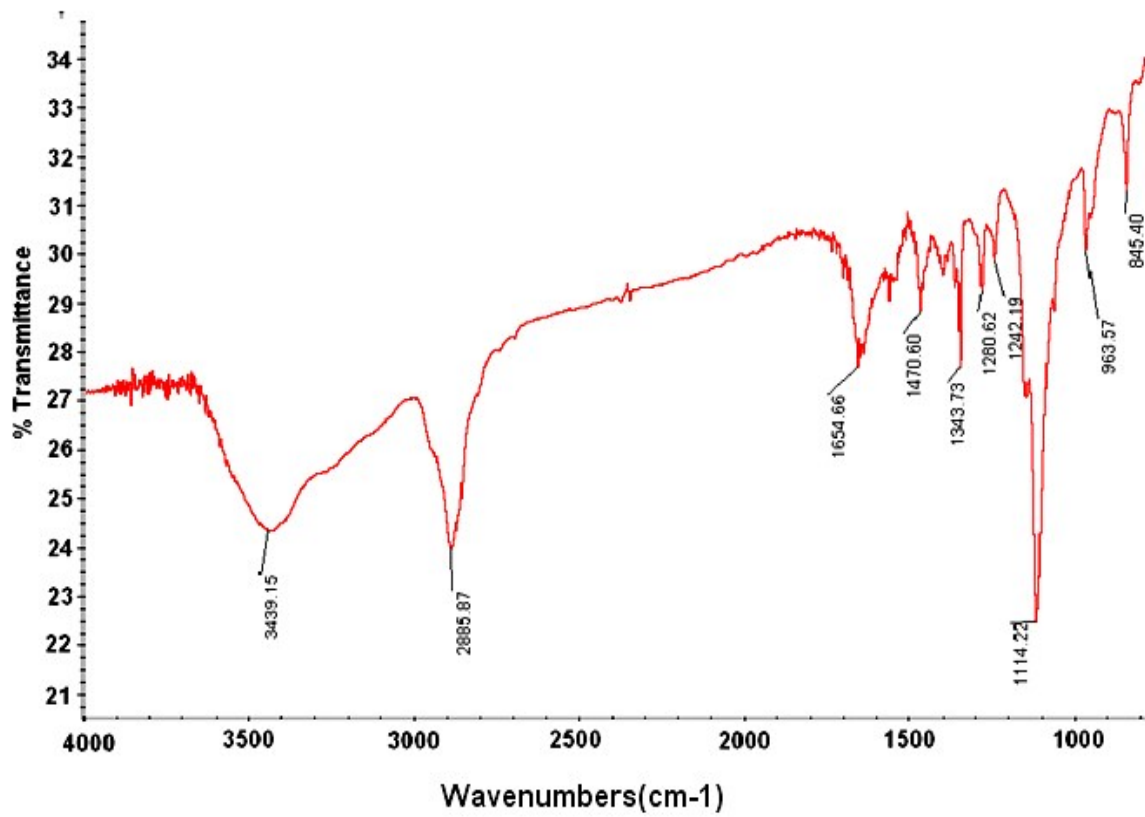


Figure S4 IR spectra of G 5.0 PAMAM

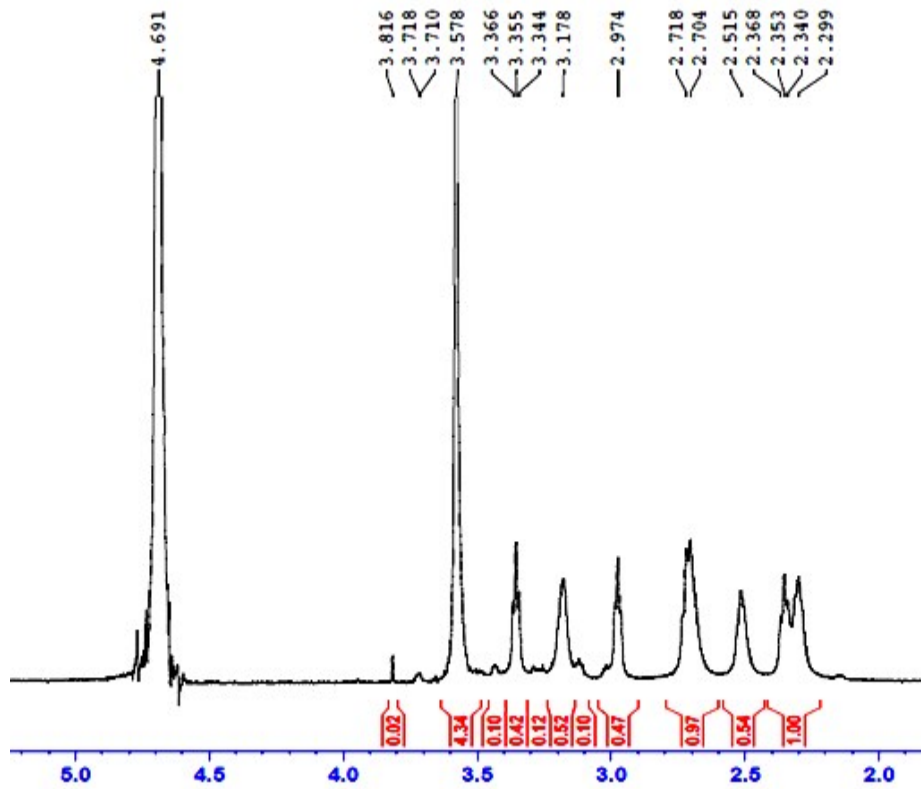


Figure S5  $^1\text{H}$  NMR spectra of PEG-G5.0 PAMAM

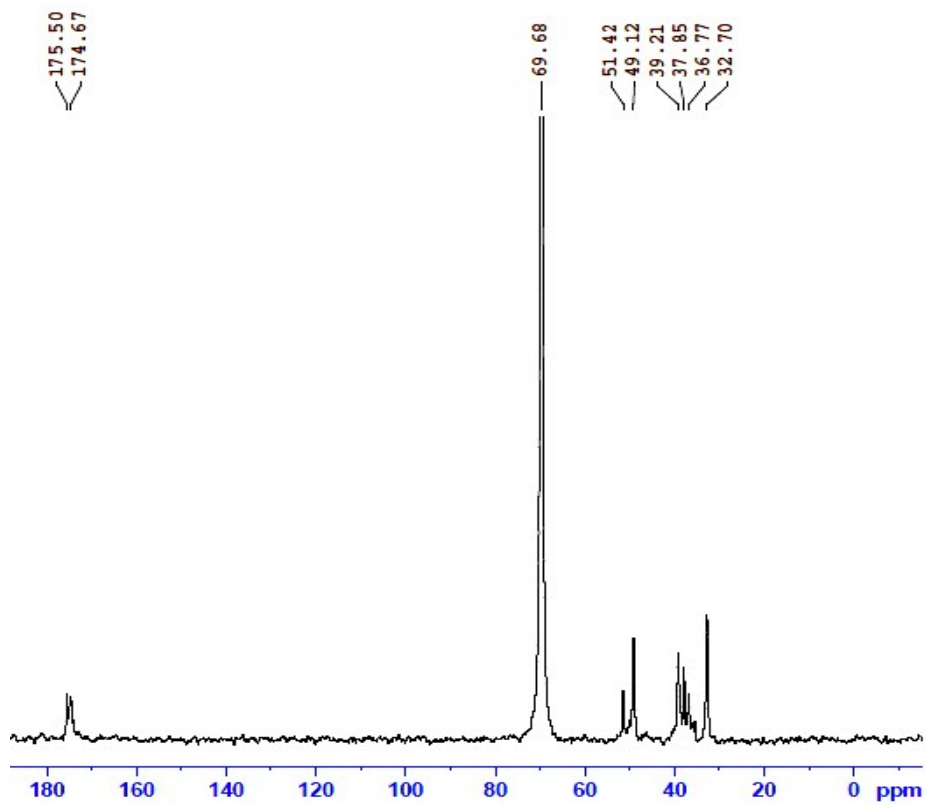
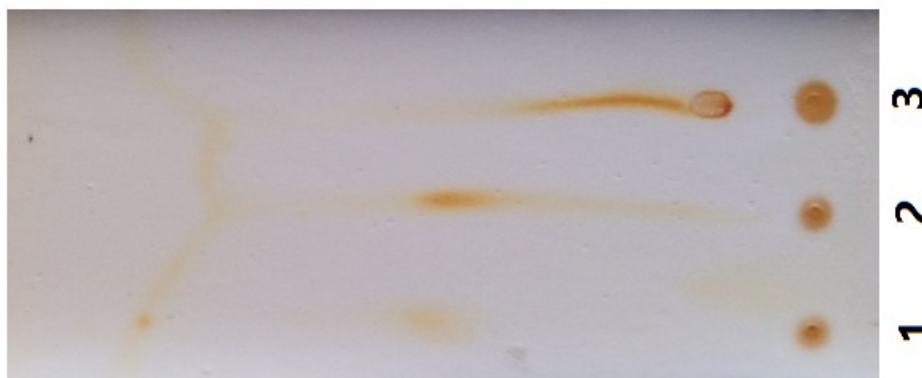
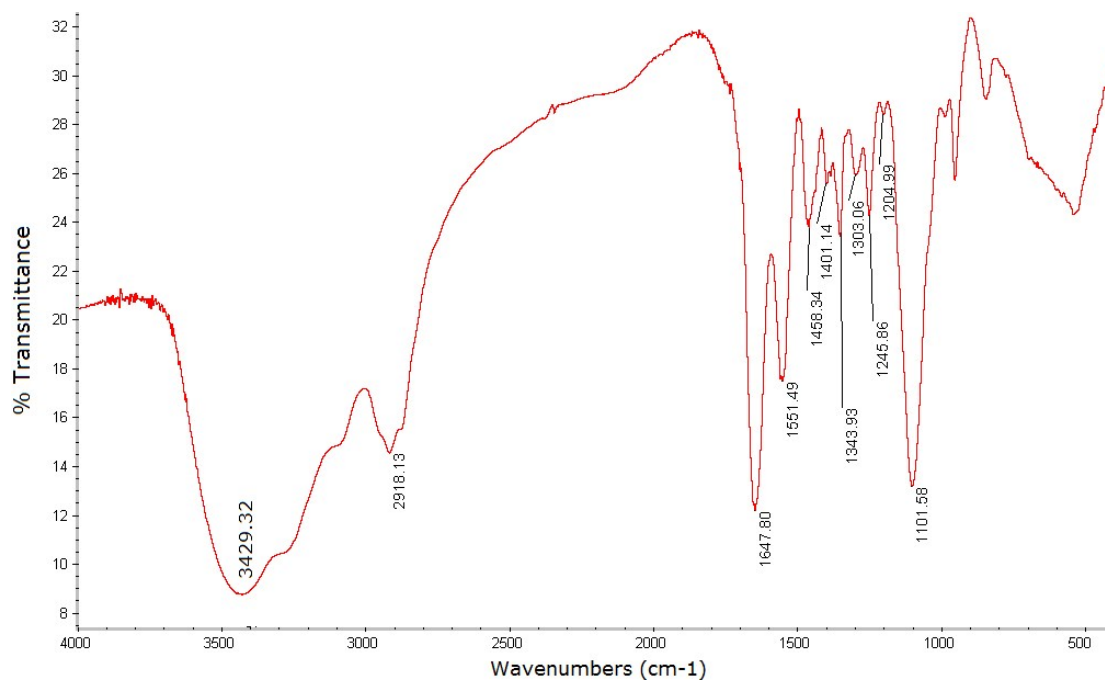


Figure S6  $^{13}\text{C}$  NMR spectra of PEG-G5.0 PAMAM



**Figure S7 Thin-Layer Chromatography (TLC) spectra of PEG-PAMAM:** chloroform-methanol (5: 1, v/v) was applied as TLC developing solvent for the separation of different components. The iodine steam was selected as chromogenic agent. G5.0 PAMAM (lane 1), PEG-G5.0 PAMAM (lane 2) and MAL-PEG<sub>3400</sub>-NHS (lane 3) were shown in this diagram, respectively.



**Figure S8 IR spectra of PEG-G5.0 PAMAM diblock copolymers.**

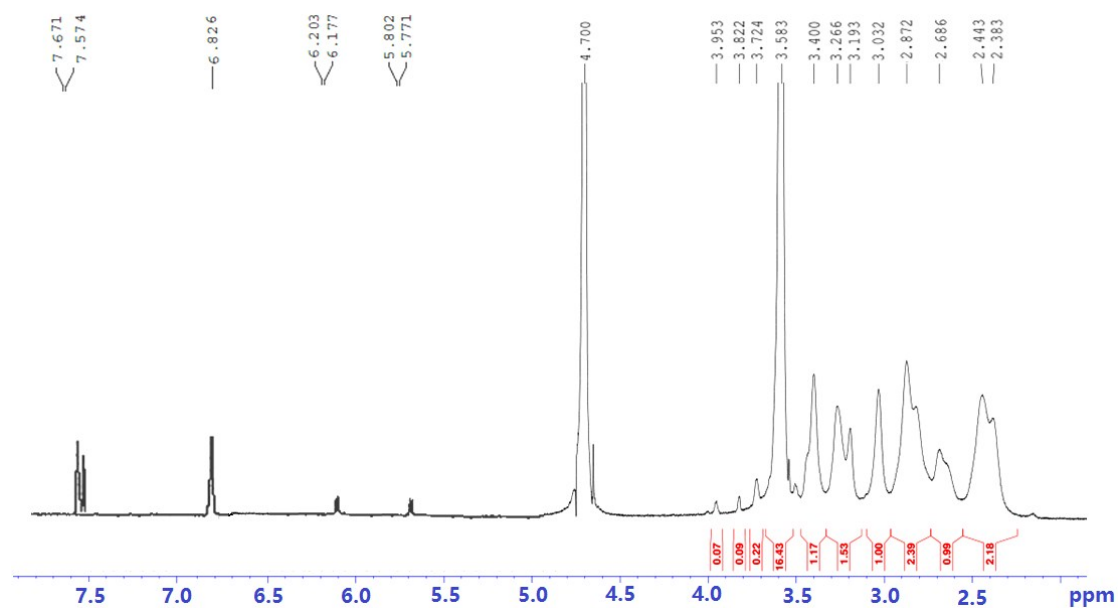


**Figure S 9**  $^1\text{H}$  NMR spectra of T7-PGD-PEG-PAMAM

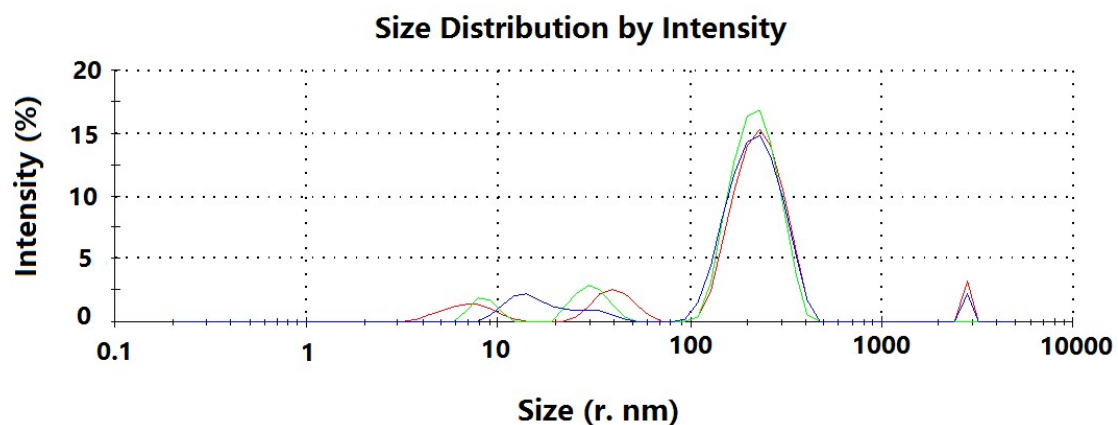


**Figure S 10** The average particle size of T7-PGD-TS II A-PEG-PAMAM NPs. Dynamic light scattering (DLS) revealed particles with diameter  $205 \pm 17$  nm.

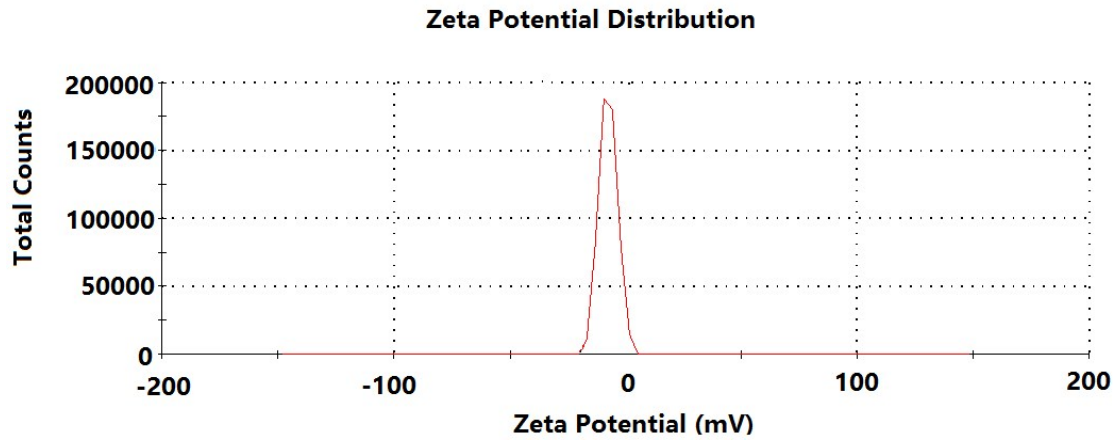


**Figure S 11** Zeta potential distribution of T7-PGP-TS II A-PEG-PAMAM NPs. T7-PGP-TS II A-PEG-PAMAM NPs feature zeta potential value (5.7 mV).

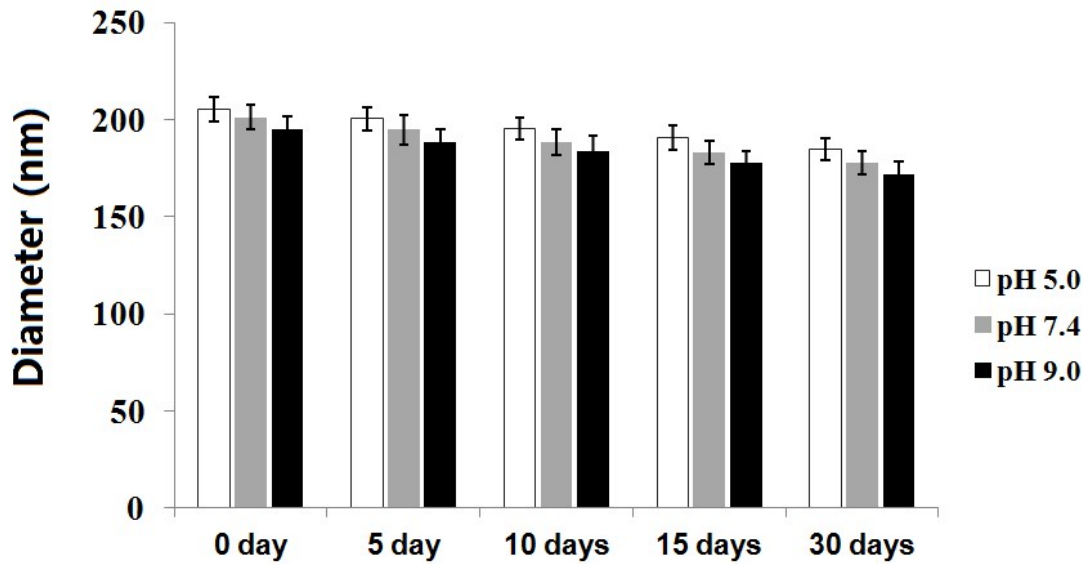


**Figure S12.** The stability of T7-PGP-TS II A-PEG-PAMAM NPs in solutions with varying pH as judged by their diameter

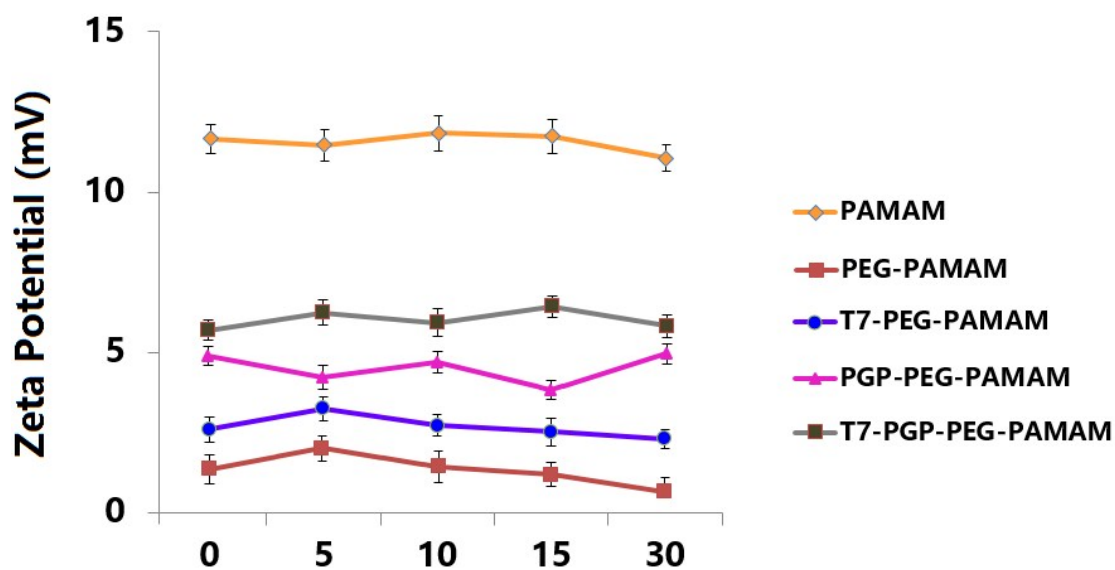


**Figure S13.** The stability of PAMAM NPs, PEG-PAMAM NPs, T7-PEG-PAMAM NPs, PGP-PEG-PAMAM NPs and T7-PGP-PEG-PAMAM NPs in solutions as judged by their zeta potential.

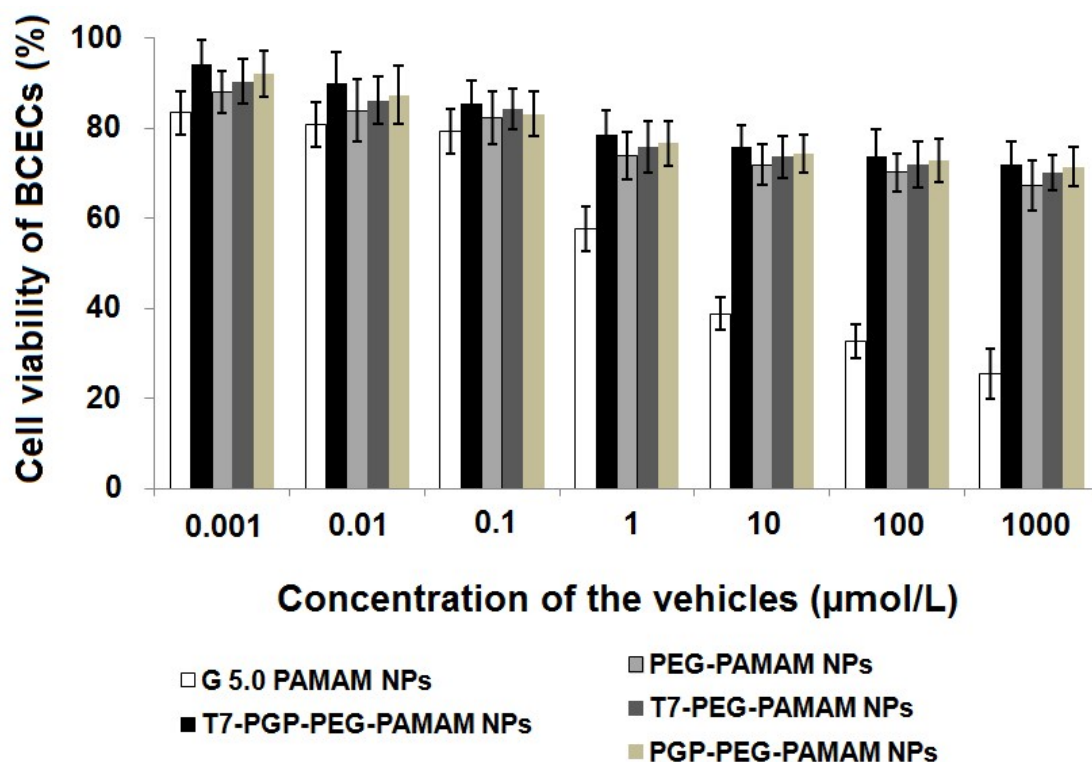
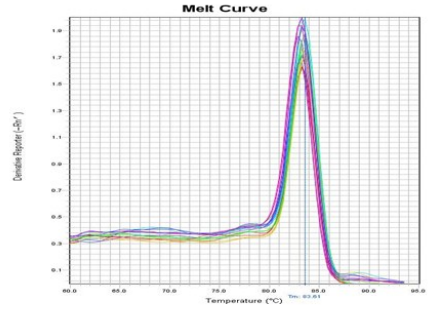
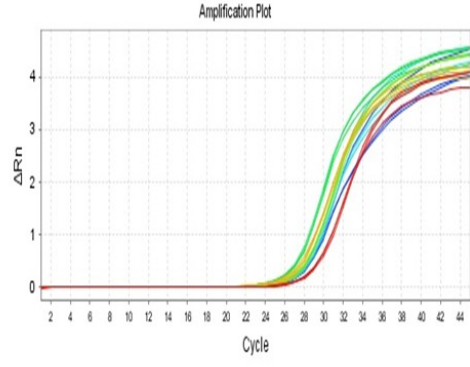


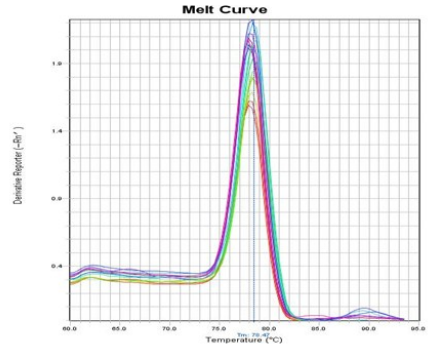
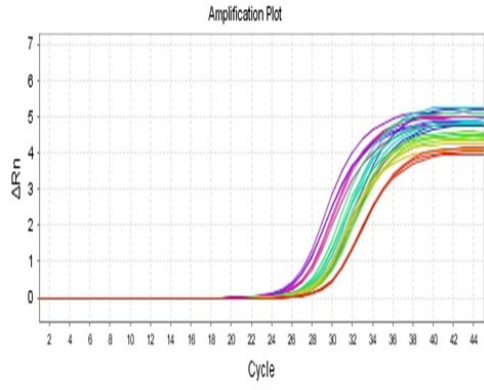
**Figure S 14** Cell viability of BCECs after treated with blank vehicles for 48 h at 37°C

**A**

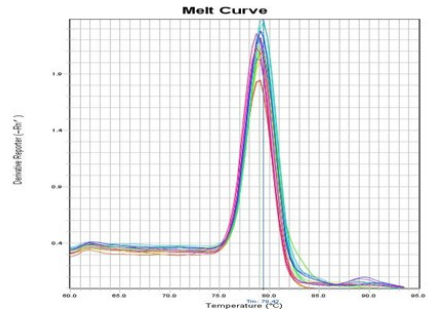
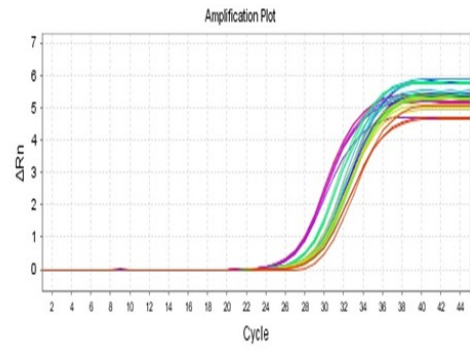
**TLR2**



**TLR3**



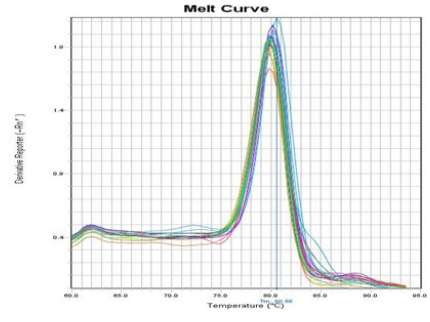
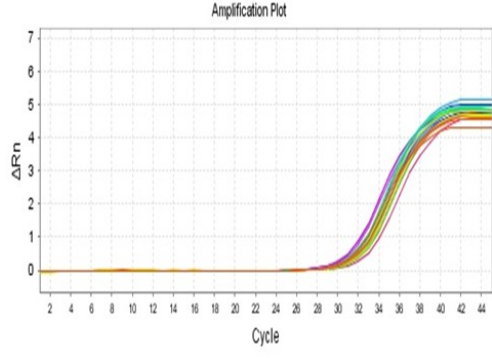
**TLR4**



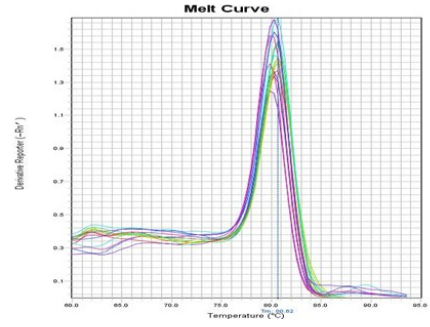
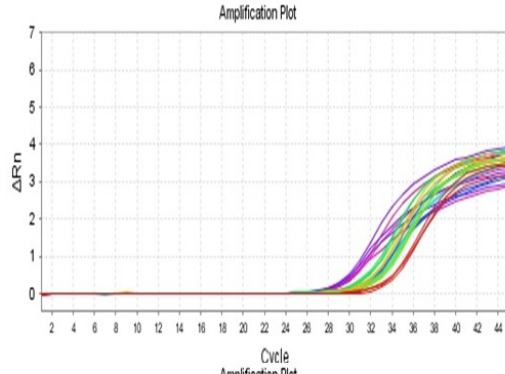


**B**

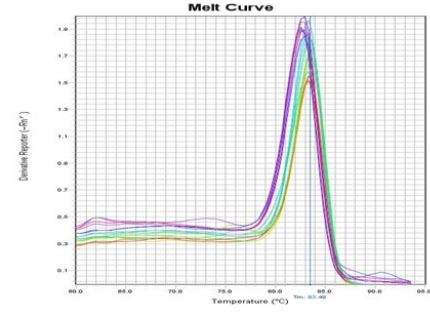
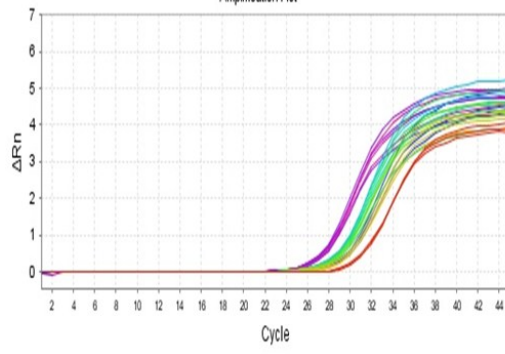
**TLR5**



**TLR9**

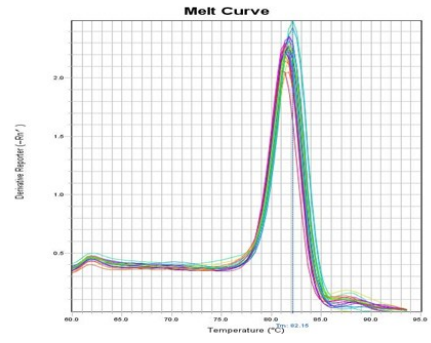
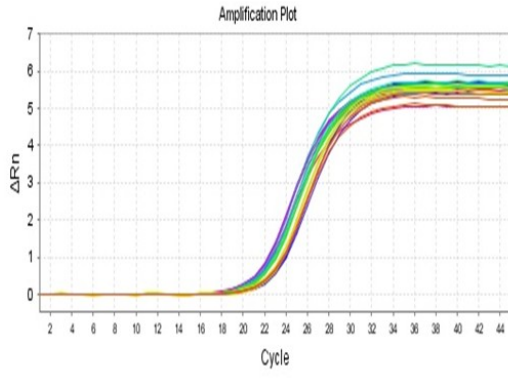


**MyD88**

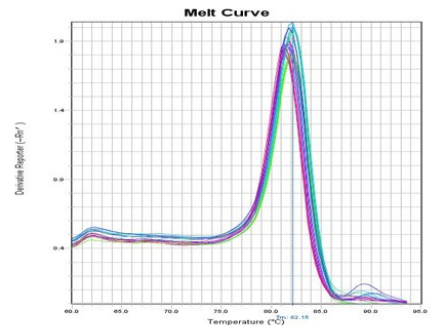
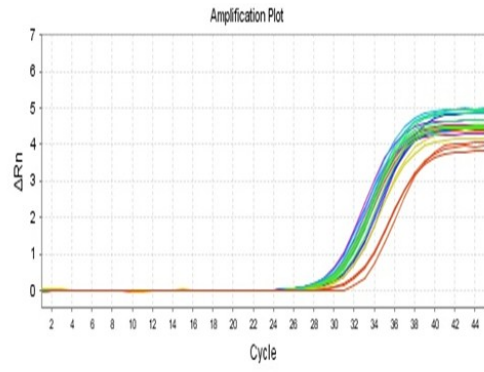


C

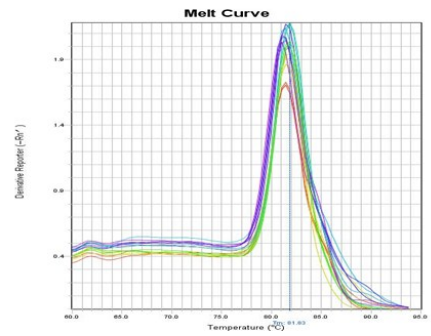
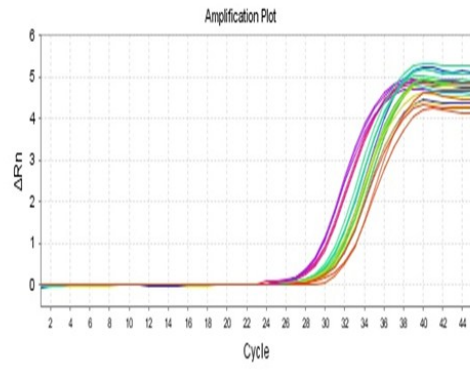
HMGB1



TRFA6



TRIF



**D**

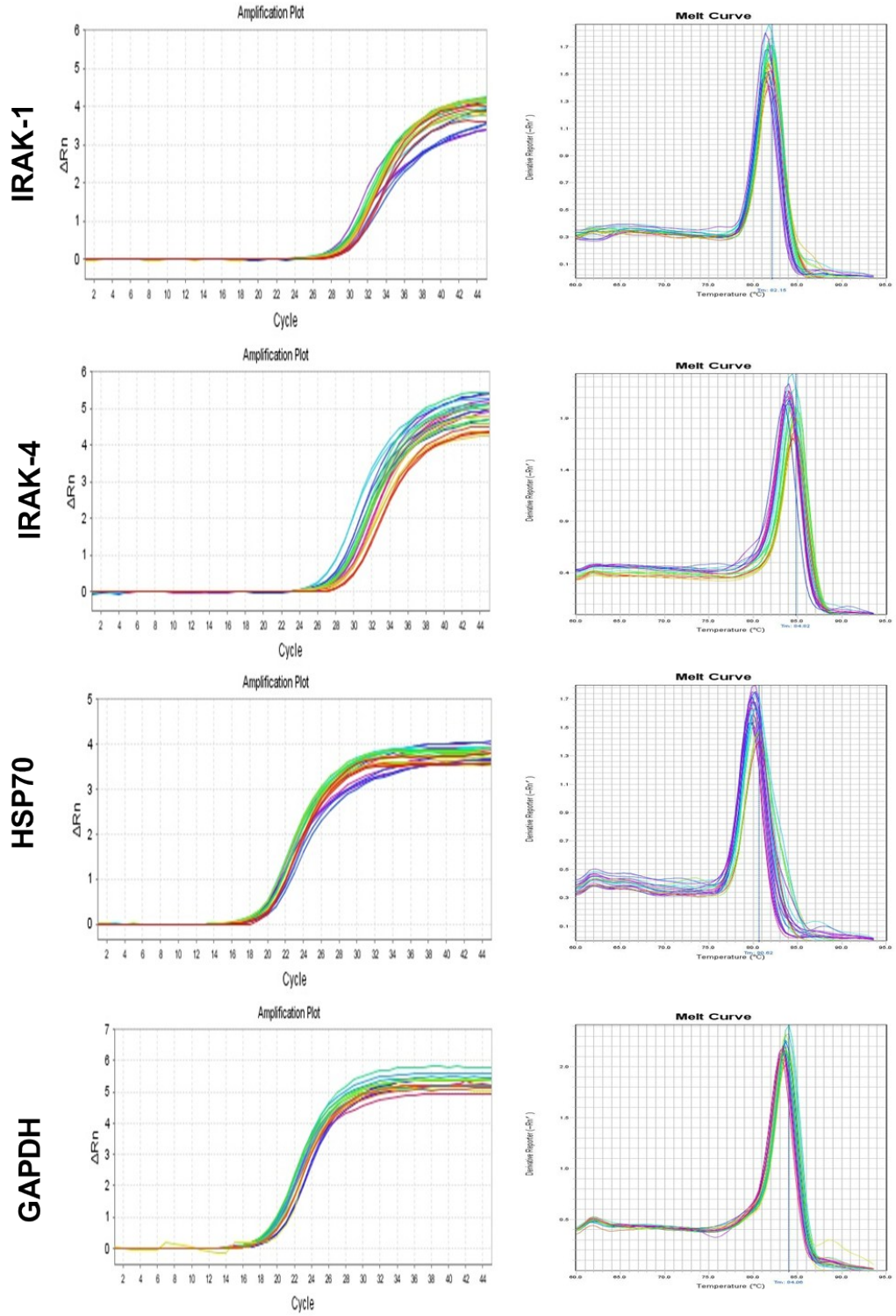


**Figure S 15** The real-time PCR amplification plots and product melt curves

**Table. S1** Sequences of the amplification primers used in the real-time PCR.

<b>mRNA Species</b>		<b>Oligonucleotides (5'→3')</b>	<b>Product size (bp)</b>
HMGB1	forward	AAGAAGTGCTCAGAGAGGTGGAAG	262
	reverse	CTAGTTTCTTCGCAACATCACCA	
MyD88	forward	TTTCGACGCCTTCATCTGCTACTGC	184
	reverse	CACCACCATGCGACGACACCTT	
IRAK-1	forward	AAGTCCATACCCGACAACAGT	168
	reverse	ATGCGAGGCAGAAGATTACC	
IRAK-4	forward	CAATGCCGCTCATCTTACCT	298
	reverse	GCTGAAGTCCCCTCCTTAGTG	
TRAF6	forward	CGCCAAAATGGAAACGCAGAG	128
	reverse	AGTTGCCAATCTTCCAATGTAAATGC	
TLR2	forward	CTGTGGTATCTGAGAATGATGTGGG	239
	reverse	TCGATGGAATCAATGATGTTGTCAA	
TLR3	forward	ACACCAGTACGCTCCTGACTTTTAT	134
	reverse	CTGCTCACCCCTGTGCATCTATTT	
TLR4	forward	CAAGACTATCATCAGTGTATCGGTGG	224
	reverse	GCTCGTTTCTCACCCAGTCCTC	
TLR5	forward	CCACCAAGGACTGCGATGAA	118
	reverse	CGGAATTTTGTGACTATGAGGG	
TLR9	forward	TGGCAGGCAATCTACTAAAGGC	98
	reverse	CACAAAGACGATACTGTTGCTACTGA	
TRAM	forward	GGCATGAGGAGCAAGCTGAAGAAG	146
	reverse	GCATGGCATCTCGGCGAAGACTAT	
TRIF	forward	CCCTGACTCTCTGGCTGCT	172
	reverse	CGGCAGAACATCGTCTCCTA	
HSP70	forward	CCACCAAGCAGACGCAGAC	111
	reverse	GCCCCAGCAGGTTGTTGTC	

GAPDH	forward	TTCCTACCCCAATGTATCCG	270
	reverse	CCACCCTGTTGCTGTAGCCATA	

**Table S2.** The main pharmacokinetic parameters of tanshinone IIA (TS II A) following intravenous administration of free TS II A, T7-TS II A-PEG-PAMAM NPs, PGP-TS II A-PEG-PAMAM NPs and T7-PGP-TS II A-PEG-PAMAM NPs.

Pharmacokinetic parameters	free TS II A	TS II A -PAMAM NPs	T7-TS II A -PEG-PAMAM NPs	PGP-TS II A- PEG-PAMAM NPs	T7-PGP- TS II A-PEG- PAMAM NPs
$t_{1/2\beta}$ (h)	0.84 ± 0.29	1.41 ± 0.77	8.54 ± 1.31	8.93 ± 1.67	9.68 ± 1.86
MRT (h)	1.65 ± 0.47	2.93 ± 0.84	11.69 ± 2.36	12.38 ± 3.52	13.86 ± 4.62
AUC <sub>0-∞</sub> (μg × h/l)	0.19 ± 0.05	0.37 ± 0.11	1.21 ± 0.39	1.43 ± 0.51	1.65 ± 0.76
CLs [L/(h kg)]	1.81 ± 0.34	1.41 ± 0.29	0.49 ± 0.14	0.41 ± 0.11	0.35 ± 0.08

## References

1. H. Guo, Q. Lai, W. Wang, Y. Wu, C. Zhang, Y. Liu and Z. Yuan, *Int J Pharm*, 2013, **451**, 1-11.
2. W. Zhang, M. W. Saif, G. E. Dutschman, X. Li, W. Lam, S. Bussom, Z. Jiang, M. Ye, E. Chu and Y. C. Cheng, *J Chromatogr A*, 2010, **1217**, 5785-5793.
3. X. Liu, C. An, P. Jin, X. Liu and L. Wang, *Biomaterials*, 2013, **34**, 817-830.
4. X. Liu, M. Ye, C. An, L. Pan and L. Ji, *Biomaterials*, 2013, **34**, 6893-6905.
5. Y. Bi, L. Liu, Y. Lu, T. Sun, C. Shen, X. Chen, Q. Chen, S. An, X. He, C. Ruan, Y. Wu, Y. Zhang, Q. Guo, Z. Zheng, Y. Liu, M. Lou, S. Zhao and C. Jiang, *ACS Appl Mater Interfaces*, 2016, DOI: 10.1021/acsami.6b05572.
6. C. Zhang, C. L. Ling, L. Pang, Q. Wang, J. X. Liu, B. S. Wang, J. M. Liang, Y. Z. Guo, J. Qin and J. X. Wang, *Theranostics*, 2017, **7**, 3260-3275.